Supplementary Information (SI)

Wettability Gradient-Driven Capillary Filling Dynamics in Architected Tapered Microchannels

Soumadip Das*[a], Vinod B. Vanarse*†[a], Omkar S. Deshmukh‡[a]

[a] *Department of Chemical Engineering, Indian Institute of Technology, Guwahati 781039, Assam, India*

∗ These authors contributed equally to this work.

† Corresponding author: `vanarse@iitg.ac.in`

‡ Corresponding author: `o.deshmukh@iitg.ac.in`

S1 Grid independence test

A mesh independence study is conducted to determine the optimal mesh size to accurately simulate olive oil capillary filling in a water-filled microchannel over a duration of 15 ms. Free triangular mesh elements are used throughout the computational domain. The study compares the average interface velocity across six mesh configurations with largest element sizes of 2.6 μm, 1.74 μm, 1.34 μm, 0.9 μm, 0.7 μm, and 0.56 μm. Fig. S1 shows the variation in the time-averaged interface velocity ($u_{\text{interface, avg}}$) with decreasing largest element size. Initially, a gradual decrease in interface velocity is observed as the element size is refined from 2.6 μm to 0.7 μm. However, when further reduced to 0.56 μm, the change in interface velocity becomes almost negligible, indicating mesh convergence. Based on these results, a largest element size of 0.7 μm is selected as the optimal configuration, which corresponds

to a total of 12,860 grid elements. This configuration provides a good balance between computational efficiency and accuracy.

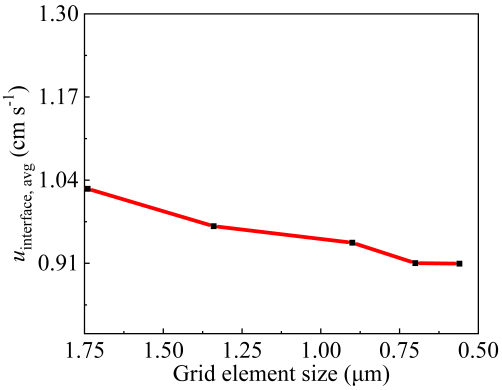

Figure S1: Variation of the average interface velocity with mesh elements over 15 ms. The values of R_1, R_3, L, and θ_w are considered as 10 μm, 2.5 μm, 200 μm, and 45°, respectively.

Table S1: Mesh settings adopted for the study.

Parameter	**Value**
Maximum element size (μm)	0.7
Minimum element size (μm)	0.02
Maximum element growth rate	1.13
Curvature factor	0.3
Resolution of narrow regions	1

Table S2: Physical properties of fluid pairs used in the capillary filling study – table captions do not end in a full point

Fluid pairs	ρ_1 (kg/m^3)	ρ_2 (kg/m^3)	μ_1 (Pa·s)	μ_2 (Pa·s)	γ (N/m)
Olive Oil–Water (OL–W)	920	1000	0.083	0.00100	0.023
Olive Oil–Seawater (OL–SW)	920	1025	0.083	0.00107	0.025
Sunflower Oil–Water (SO–W)	920	1000	0.054	0.00100	0.023
Sunflower Oil–Seawater (SO–SW)	920	1025	0.054	0.00107	0.025

S2 Convergence tolerence study

We compared the interface velocity results using convergence tolerances of 0.005 and 1×10^{-6}. As shown in Figure S2, the differences were negligible, with deviations remaining well within

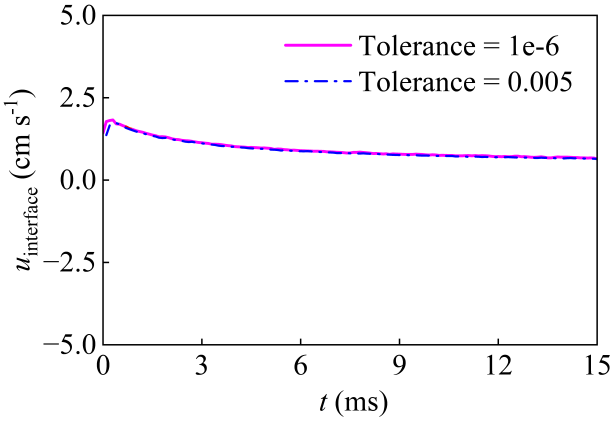

Figure S2: Comparison of capillary filling dynamics obtained with convergence tolerances of 0.005 and 1×10^{-6}. The values of R_1, R_3, L, and θ_w are taken as 10 μm, 2.5 μm, 250 μm, and 45°, respectively.

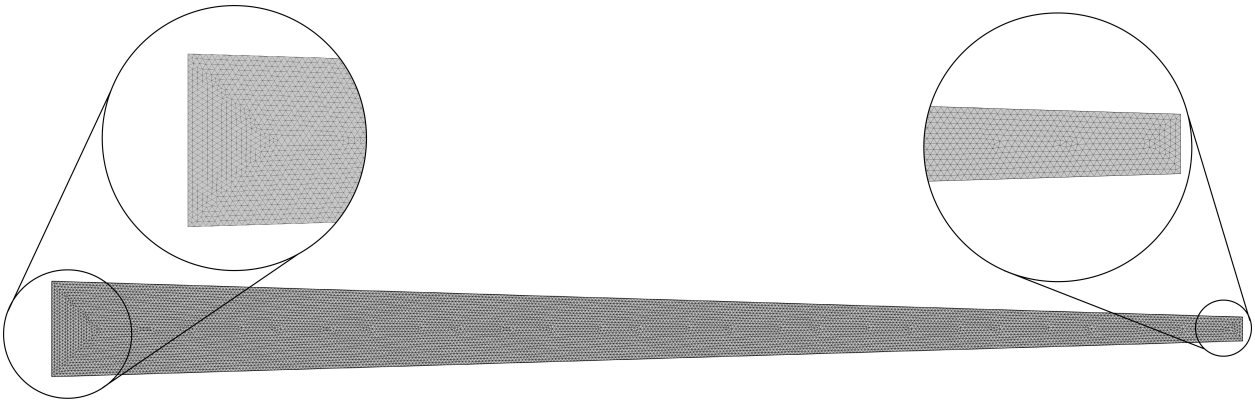

Figure S3: Representative mesh used in the study. The figure shows the computational domain discretized with triangular elements along with a zoomed-in view of the inlet and outlet regions.

1%. This indicates that further tightening the tolerance to 1×10^{-6} would substantially increase computational cost without any meaningful gain in accuracy. Therefore, we find that a tolerance of 0.005 is both reasonable and efficient for the present study.

S3 Mesh details

The mesh settings adopted in this study, corresponding to a total of 12,860 grid elements, are listed in Table S1. Free triangular elements are employed throughout the entire computational domain, with a maximum element size of 0.7 μm. A schematic representation of the

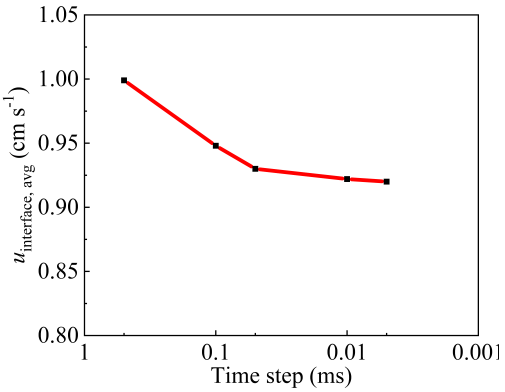

Figure S4: Variation of the time-averaged interface velocity with maximum time steps of 0.5 s, 0.1 s, 0.05 s, 0.01 s, and 0.005 s over 15 s. The geometric parameters are $R_1 = 10$ μm, $R_3 = 2.5$ μm, $L = 200$ μm, and $\theta_w = 45°$.

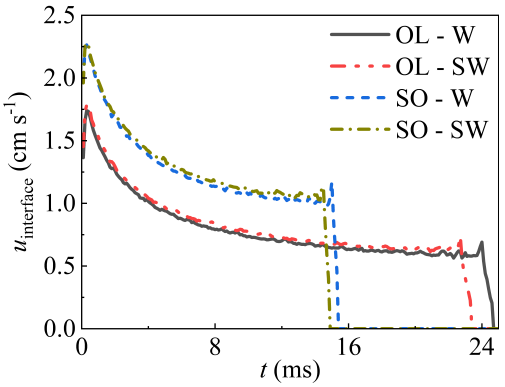

Figure S5: Plot of the temporal evolution of $u_{\text{interface}}$ for capillary filling with different fluid combinations: olive oil–water (OL-W), olive oil–seawater (OL-SW), sunflower oil–water (SO-W), and sunflower oil–seawater (SO-SW). The values of R_1, R_3, L, and θ_w are considered as 10 μm, 2.5 μm, 200 μm, and 45°, respectively.

mesh arrangement, including a zoomed-in view of the inlet and outlet regions, is shown in Fig. S3.

S4 Time step selection

The simulations employ an adaptive time-stepping scheme, where the time step is not fixed but automatically adjusted by COMSOL. A maximum allowable time step is prescribed by the user, and COMSOL reduces it as needed in regions of rapid transients or sharp gradients to maintain numerical stability and accuracy. To determine a suitable maximum allowable

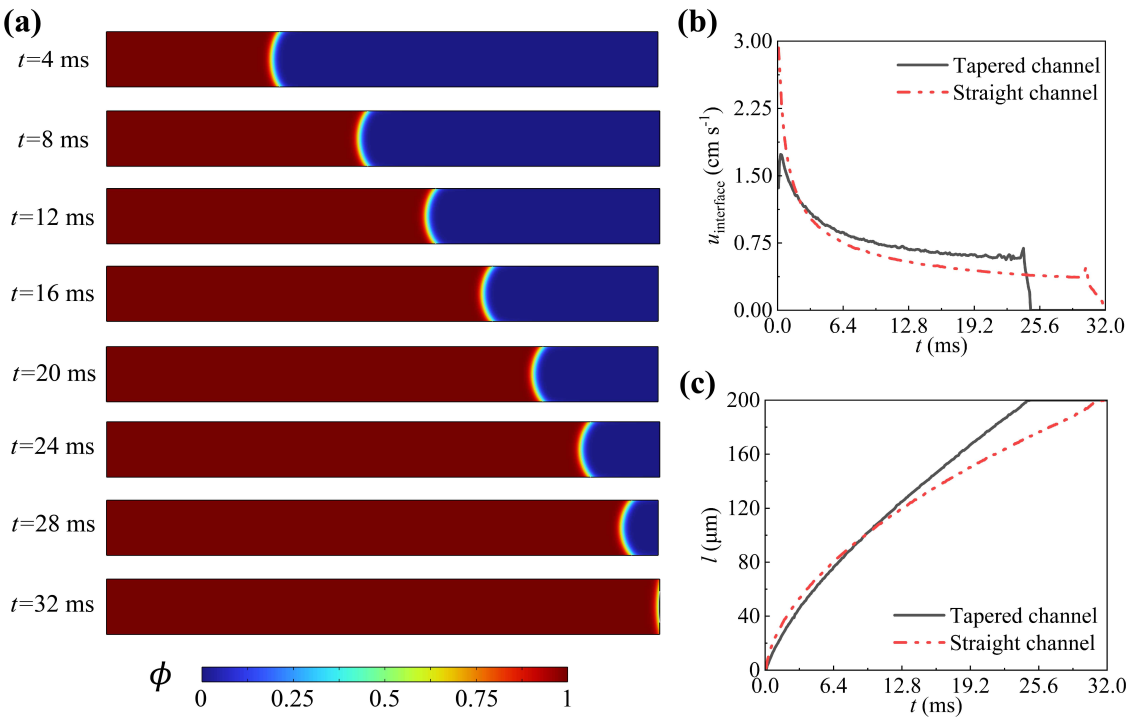

Figure S6: Representation of capillary filling of olive oil in a water-filled straight microchannel with a uniform wall contact angle. Plot (a) depicts the ϕ contours at various time intervals for $t = 4 - 32$ ms for the straight microchannel. Plots (b) and (c) compare the temporal evolution of $u_{\text{interface}}$ and l, respectively, for the straight microchannel with that of the tapered microchannel. The parameters are set as $R_1 = 10$ μm, $L = 200$ μm, and $\theta_w = 45°$, while $R_3 = 10$ μm for the straight microchannel and $R_3 = 2.5$ μm for the tapered microchannel.

time step, a time-step independence study was carried out by prescribing maximum time steps of 0.5 s, 0.1 s, 0.05 s, 0.01 s, and 0.005 s in separate simulations for capillary filling up to 15 s. In each case, COMSOL automatically reduced the time step locally whenever required by the solver. The variation of the time-averaged interface velocity for these cases is shown in Fig. S4 . The results indicate negligible variation, with the velocity remaining within the narrow range of 0.92–1.00 cm s^{-1}. In particular, reducing the maximum time step from 0.01 s to 0.005 s produced no significant change, confirming temporal convergence. Based on these results, a maximum allowable time step of 0.01 s was selected for the present study, providing an appropriate balance between computational efficiency and numerical accuracy.

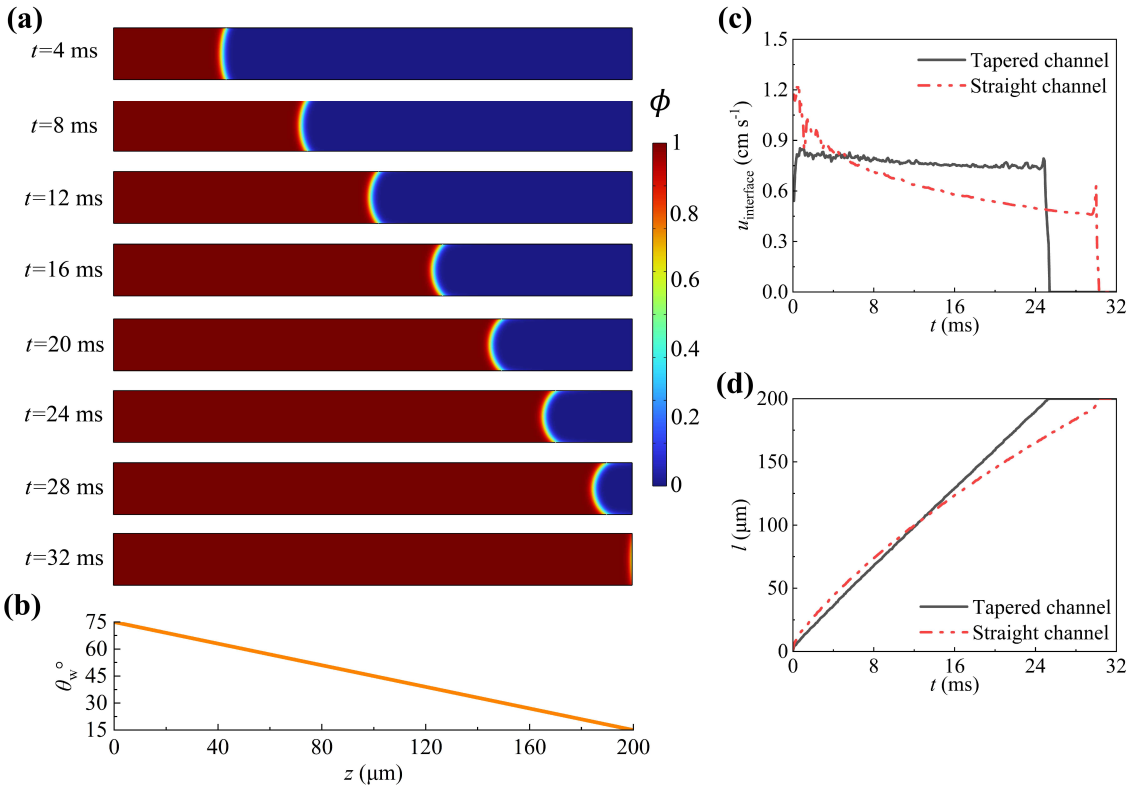

Figure S7: Straight microchannel with a linearly varying wall contact angle. Plot (a) depicts the ϕ contours at various time intervals for $t = 4 - 32$ ms for the straight microchannel. Plot (b) displays the axial variation of θ_w along the microchannel length. Plots (c) and (d) compare the temporal evolution of $u_{\text{interface}}$ and l, respectively, for the straight microchannel with that of the tapered microchannel. The parameters are set as $R_1 = 10$ μm and $L = 200$ μm, while $R_3 = 10$ μm for the straight microchannel and $R_3 = 2.5$ μm for the tapered microchannel.

S5 Results for different fluid pairs

This section investigates the impact of different fluid combinations on autonomous capillary filling in a microchannel, building upon the primary analysis presented in the main manuscript, which considered olive oil displacing water (OL-W). Here, three additional fluid pairs are examined: olive oil displacing seawater (OL-SW), sunflower oil displacing water (SO-W), and sunflower oil displacing seawater (SO-SW). The physical properties of all fluids are summarized in Table S2, and the corresponding interface velocities for each case are presented in Fig. S5. The results demonstrate that the viscosity of the displacing fluid significantly influences the interface velocity, thereby playing a crucial role in capillary fill-

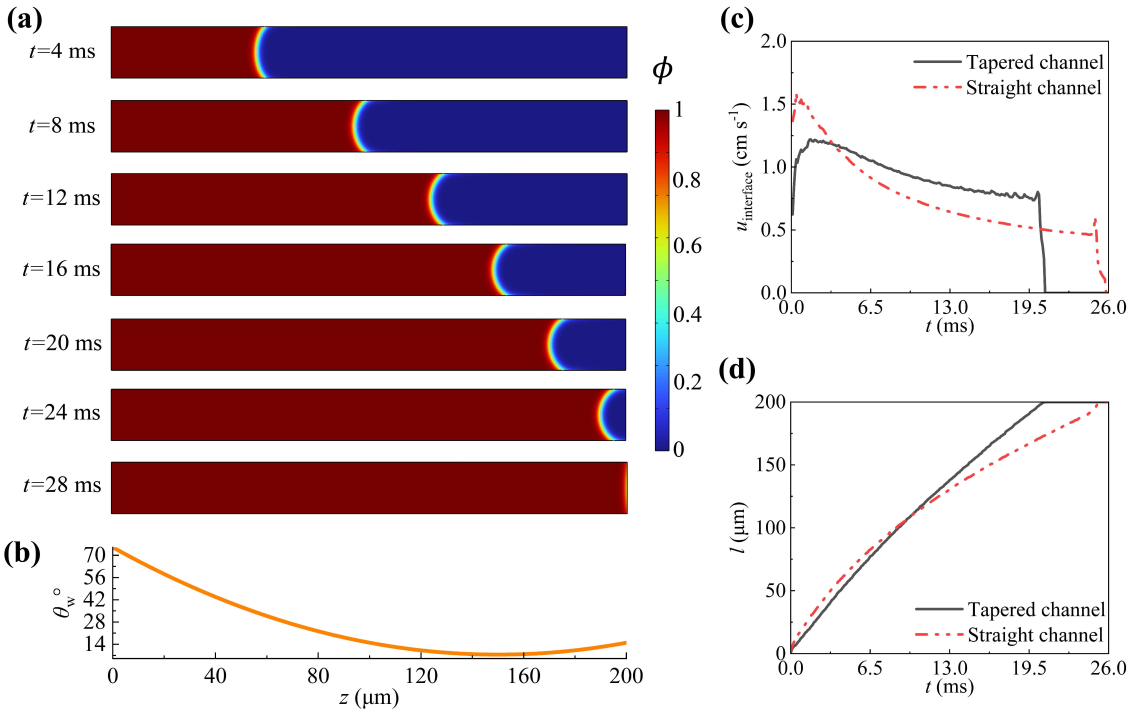

Figure S8: Straight microchannel with a quadratically varying wall contact angle. Plot (a) depicts the ϕ contours at various time intervals for $t = 4-28$ ms for the straight microchannel. Plot (b) displays the axial variation of θ_w along the microchannel length. Plots (c) and (d) compare the temporal evolution of $u_{\text{interface}}$ and l, respectively, for the straight microchannel with that of the tapered microchannel. The parameters are set as $R_1 = 10$ μm and $L = 200$ μm, while $R_3 = 10$ μm for the straight microchannel and $R_3 = 2.5$ μm for the tapered microchannel.

ing dynamics. Sunflower oil, with a lower viscosity than olive oil, consistently yields higher interface velocities and shorter displacement times. This trend aligns with the theoretical prediction from Eq. (9), which indicates an inverse dependence of interface velocity on both μ_1 and μ_2. The effect of the displaced fluid is comparatively less pronounced due to the minimal viscosity difference between water and seawater. However, variations in interfacial surface tension become important in this regime. Seawater, having a higher interfacial tension with oils, enhances the capillary driving force and thus results in a slightly faster interface advancement within the microchannel.

S6 Results for a Straight microchannel

This section further validates the claim that tapered channels achieve higher flow velocities for autonomous capillary filling compared to straight microchannels. To illustrate this, a straight microchannel with a constant diameter is analyzed under both uniform and non-uniform wettability conditions. The results are then systematically compared with those of the tapered microchannel configuration.

S6.1 Uniform Wall Wettability

Fig. S6(a) presents the ϕ contours at different time intervals during the capillary filling process, illustrating the progression of the fluid interface in a straight microchannel. Similar to the tapered geometry with uniform wall wettability, olive oil displaces water; however, the interface dynamics differ significantly due to geometric effects. In both straight and tapered microchannels, the deceleration of the fluid front is driven by increasing viscous dissipation as the higher-viscosity olive oil advances. In the straight microchannel, this velocity reduction is more pronounced, following the classical Lucas–Washburn regime where velocity decays as $1/\sqrt{t}$ due to growing viscous resistance over the penetration length[1–4]. The absence of a taper-induced pressure gradient, which sustains motion against viscous drag in the tapered case, exacerbates this slowdown. This observation is supported by Fig. S6(b) and S6(c), which compare the temporal evolution of interface velocity and position, respectively, for both geometries. Initially, the interface in the straight microchannel moves faster due to the uniform cross-section, which offers lower flow resistance. However, as olive oil progresses, the velocity decreases more sharply compared to the tapered channel, where the narrowing geometry generates an increasing capillary pressure gradient to counter the rising viscous resistance, leading to a velocity plateau. This comparison highlights the critical role of geometric tapering in enhancing capillary filling dynamics. By analyzing these differences in interface dynamics and velocity profiles, the advantages of tapered geometries

become evident, particularly in applications requiring consistent flow rates and controlled fluid motion.

S6.2 Non-Uniform Wall Wettability

This section analyzes the dynamics of capillary filling in a straight microchannel under linear and quadratic variations of the wall contact angle. The results are then compared with those of the tapered microchannel under analogous conditions. For the linear variation scenario, the wall contact angle changes axially according to Eq. (22), whereas for the quadratic variation scenario, it follows Eq. (23), as given in the main manuscript. Fig. S7(a) and Fig. S8(a) present the ϕ contours at different time intervals during the capillary filling process for linearly and quadratically varying contact angles, respectively, in the straight microchannel. Similar to the uniform contact angle case, it is observed that the interface velocity decreases over time in the straight microchannel, and the time required to reach the outlet increases significantly in both scenarios. This behavior is further reinforced by Fig. S7(c-d) and Fig. S8(c-d), which depict the interface dynamics for the linear and quadratic cases, respectively. While the tapered microchannel maintains a relatively uniform velocity of the leading interface, the straight microchannel exhibits a significant reduction in velocity as the fluid progresses. This highlights the inefficiency of straight microchannels in achieving consistent flow velocity, a critical requirement for many industrial applications. The absence of an additional pressure drop, which is inherently provided by the tapering geometry, further exacerbates this limitation. Consequently, straight microchannels are less suitable for applications requiring constant throughput, underscoring the advantages of tapered geometries in enhancing capillary filling dynamics and ensuring reliable performance in microfluidic systems.

References

[1] E. W. Washburn, Physical Review, 1921, **17**, 273–283.

[2] L. Hanžič, L. Kosec and I. Anžel, Cement and Concrete Composites, 2010, **32**, 84–91.

[3] J. André and K. Okumura, Langmuir, 2020, **36**, 10952–10959.

[4] J. Cai, Y. Chen, Y. Liu, S. Li and C. Sun, Advances in Colloid and Interface Science, 2022, **304**, 102654.